

Substituent Effect on the Electronic Properties and Morphologies of Self-Assembling Bisphenazine Derivatives

Kelly K. McGrath, Kyoungmi Jang, Kathleen A. Robins, and Dong-Chan Lee*^[a]

Abstract: This paper reports the synthesis and characterization of novel self-assembling *n*-type organic semiconductors based on asymmetrically substituted bisphenazines with various functional groups of different size, electron-withdrawing ability, and conjugation length. The overarching objective of this research is to tune electronic properties and morphologies of self-assembled structures of this system simultaneously, which offers a potentially useful platform for future optoelec-

tronic applications. The thermal, optical, and electrochemical properties associated with different substituents were studied by differential scanning calorimetry (DSC), UV-visible and fluorescence spectroscopy, and cyclic voltammetry (CV). Electronic properties were calculated using density func-

tional theory, and results were compared to experimental HOMO, LUMO, and energy gaps. The one-dimensional (1D) self-assembly properties of these new *n*-type molecules are discussed in terms of the type of peripheral substituents, alkyl side group length, and assembly conditions. This study includes extensive investigations by scanning electron microscopy (SEM) and X-ray diffraction (XRD).

Keywords: electronic properties • morphology • nanostructures • self-assembly • semiconductors

Introduction

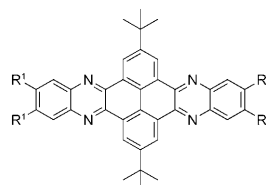
The 1D self-assembly of π -conjugated organic semiconductors^[1] into well-defined superstructures with high aspect ratios has been one of the most exciting research areas in recent years. These systems are of interest primarily because of their potential application in nanoscale electronic devices.^[2] Diverse molecular systems have been reported, which show a variety of 1D nanostructures. A popular design approach involves the synthesis of large π -cores with solubilizing side groups, maximizing intermolecular π -orbital overlap as a driving force for assembly.^[1a] Controlling the morphologies of nanostructures is particularly important as many properties are dependent on molecular packing.^[3] To that end, the manipulation of solubilizing alkyl side groups bonded to π -cores has been the most rigorously studied to date.^[4]

Meanwhile, tuning the electronic properties of π -cores including the band gap,^[5] as well as the HOMO and LUMO energy levels, by introducing peripheral substituents such as cyano^[6] or fluorine^[7] is equally as important as morphology control. These structural modifications are much more facile and convenient than designing a new π -core, which likely entails new and complex synthetic routes. Although peripheral substituent effects on some π -cores have been extensively studied, in most cases, the major focus has been electronic properties. Several current studies demonstrate the role of peripheral substituents on the molecular assembly, however, they primarily concentrated on the crystalline form^[3c,6f] or surface based assembly.^[8]

In a recent communication,^[9] we reported an organogelator based on a bisphenazine asymmetrically substituted with acetylene and hexadecyloxy groups (compound **1** in Scheme 1). We found that belt-shaped 1D nanofibers were

[a] K. K. McGrath, K. Jang, Prof. K. A. Robins, Prof. D.-C. Lee
Department of Chemistry
University of Nevada Las Vegas
4505 Maryland Parkway, Box 454003
Las Vegas, Nevada 89154-4003 (USA)
Fax: (+1) 702-895-4072
E-mail: Dong-Chan.Lee@unlv.edu

Supporting information for this article is available on the WWW under <http://dx.doi.org/10.1002/chem.200802148>.



- 1: R¹ = —H, R² = OC₁₆H₃₃
- 2: R¹ = H, R² = OC₁₆H₃₃
- 3: R¹ = F, R² = OC₁₆H₃₃
- 4: R¹ = I, R² = OC₁₆H₃₃
- 5: R¹ = NO₂, R² = OC₁₆H₃₃
- 6: R¹ = NO₂, R² = OC₁₂H₂₅

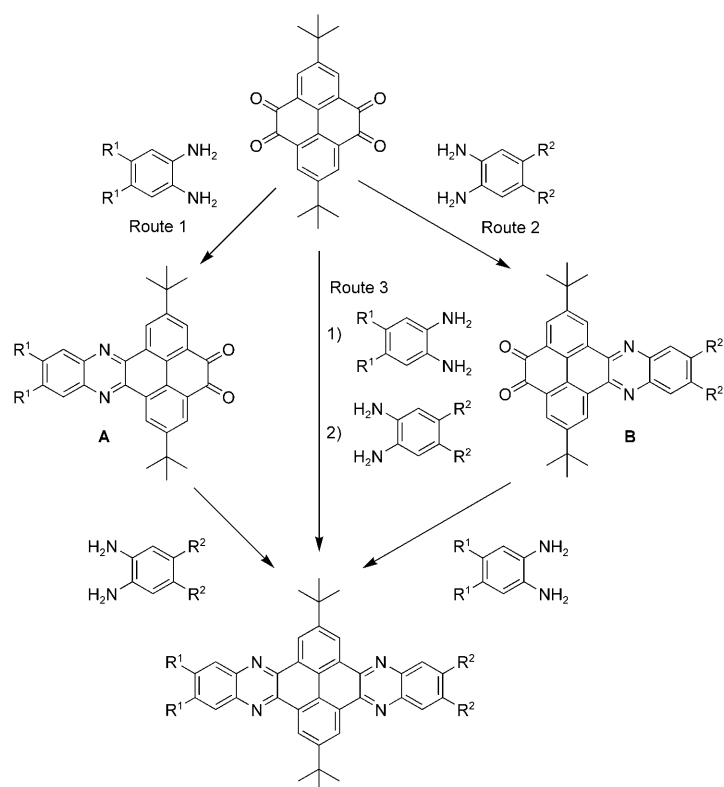
Scheme 1. Asymmetrically substituted bisphenazine derivatives.

grown in select solvents via the cooperative interplay of π - π interaction, hydrogen bonding, and van der Waals interaction. This design approach enabled us to introduce various substituents directly onto the bisphenazine core. In this paper, we aim to achieve not only well-defined 1D nanostructures of the new *n*-type semiconductors, but also the ability to tune the electronic properties of the heteroaromatic moiety without compromising the assembling ability. Three major structural features are of importance in this design. First, bisphenazine is a large, heteroaromatic molecule that promotes self-assembly through its large flat π -core.^[10] In addition, the presence of four imine nitrogen groups makes the ring electron-deficient^[11] creating a potentially useful electron transporting material. We are particularly interested in developing new *n*-type organic semiconductors, which are relatively scarce when compared to *p*-type. The importance of self-assembling *n*-type molecules has been substantiated by a number of studies.^[3b,10,12] Secondly, the peripheral substituents (R^1) added to one side of the π -core vary in size, electron-withdrawing ability, and conjugation length. These substituents will further tune the electronic properties, such as electron-deficiency and HOMO-LUMO energy gap, while modulating the morphology of the assembly. Third, two long alkoxy chains (R^2) added to the other side of the π -core promote solubility and assembly through cooperative van der Waals interactions. Growth of the nanoclusters in the direction of the alkoxy side group may be inhibited by the local interactions between solvent and side chain while the long axis growth will be favored by π - π stacking. A thorough investigation of the effect of the following parameters on either electronic or assembly properties or both will be discussed: the type of peripheral substituents, the length of alkoxy side groups, assembly methodology, and the types of solvent system used for assembly.

Results and Discussion

The title compounds (**2–6**) were prepared by either stepwise cyclization or sequential addition using 2,7-di-*tert*-butylpyrene-4,5,9,10-tetraone and two different *o*-diaminoarenes to generate asymmetric bisphenazine.

Compound **4** was tested with the stepwise cyclization (Route 1 and 2 in Scheme 2) and sequential addition (Route 3). In Route 1, the insolubility of intermediate **A** hampered its purification, thus resulting in a low yield in the second cyclization. On the other hand, Route 2 produced the soluble intermediate **B** which could successfully be purified with silica gel column chromatography, generating a reasonable yield for the two step reaction ($\approx 50\%$). As a result, Route 2 was used for the synthesis of final compounds **2–5**, owing to the flexibility of structural modification. Although Route 3 involved the least number of steps, the yields were inconsistent and low depending on the type of R^1 if R^2 was hexadecyloxy group ($<35\%$). Interestingly compound **6**, which contains the dodecyloxy group, produced a comparable



Scheme 2. Stepwise cyclization (Routes 1 and 2) and sequential addition (Route 3) to asymmetric bisphenazine derivatives.

yield when either Route 2 or 3 was used. Therefore, compound **6** was synthesized by using Route 3. Compound **1** was synthesized from compound **4** according to the previous report.^[9]

The UV-visible absorption spectra for compounds **1–5** are shown in Figure 1. All of the compounds showed λ_{\max} near 418 and 422 nm arising from the bisphenazine core. The spectra of **1** and **4** have shoulders near $\lambda = 450$ nm, owing to increased conjugation with the acetylene and iodine, respectively. The λ_{\max} of compound **5** was slightly blue-shifted to 396 and 418 nm in comparison to the other compounds, however, the shoulder was broadened and red-shifted to $\lambda = 468$ nm. The greater shift of the shoulder in **5** may be a

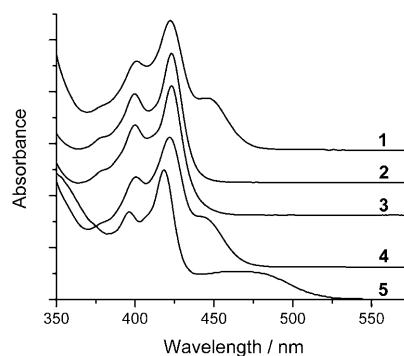


Figure 1. UV-visible spectra of compounds **1–5** (absorption of compound **6** is identical to that of compound **5**).

result of more extensive conjugation with the NO₂ groups. We note that the absorption spectra of compounds **5** and **6** are nearly identical, which was anticipated because changing the alkyl chain length of the side groups should not affect the chromophore. The absorption of all the compounds, including the shoulders at longer wavelengths, followed Beer's law, which ruled out any absorption induced by molecular aggregation. The absorption edge was gradually shifted to longer wavelengths as the peripheral substituent was changed from H (**2**) to F (**3**) to I (**4**) to acetylene (**1**) to NO₂ (**5** and **6**). As a result, the HOMO–LUMO energy gap calculated from the tangent of the absorption edge^[13] decreased in the same order (Table 1). The experimental esti-

Table 1. Electronic properties of compounds **1–6** from experiments and theoretical calculation.

	$E_{\text{red}}^{\text{peak}}$ [V]	$E_{\text{red}}^{\text{onset}}$ [V]	$E_{\text{LUMO}}^{\text{[a]}}$ [eV]	$E_{\text{HOMO}}^{\text{[b]}}$ [eV]	$E_{\text{gap}}^{\text{[c]}}$ [eV]	$E_{\text{LUMO}}^{\text{[d]}}$ [eV]	$E_{\text{HOMO}}^{\text{[d]}}$ [eV]	$E_{\text{gap}}^{\text{[d]}}$ [eV]
1	-1.68	-1.53	-3.27	-5.84	2.57	-2.66	-5.75	3.09
2	-1.81	-1.68	-3.12	-5.86	2.74	-2.39	-5.69	3.30
3	-1.76	-1.63	-3.17	-5.88	2.71	-2.61	-5.80	3.19
4	n/a ^[e]	n/a ^[e]	n/a ^[e]	n/a ^[e]	2.58	n/a ^[f]	n/a ^[f]	n/a ^[f]
5	-1.14	-1.03	-3.77	n/a ^[g]	n/a ^[g]	-3.39	-6.10	2.71
6	-1.14	-1.03	-3.77	n/a ^[g]	n/a ^[g]	-3.39	-6.10	2.71

[a] $E_{\text{LUMO}} = -(E_{\text{red}}^{\text{onset}} + 4.8 \text{ eV})$. [b] $E_{\text{HOMO}} = E_{\text{LUMO}} - E_{\text{gap}}^{\text{optical}}$. [c] Optical HOMO–LUMO energy. [d] Theoretical calculation. [e] Peak potentials for **4** were not clearly resolved. [f] Theoretical treatment for **4** was not carried out, owing to limitations in suitably packaged basis sets for iodine. [g] Evaluation of experimental E_{gap} from UV-visible spectroscopy was not clearly resolved, owing to long tailing of the absorption edge. As a result, experimental E_{HOMO} was not estimated.

mation of HOMO–LUMO energy gaps of compounds **5** and **6** was not clearly resolved, owing to long tailing of the absorption edge. However, our early estimation indicated that the energy gaps for **5** and **6** are identical to each other, and are smaller than those of the other compounds listed in Table 1. The UV-visible absorption results showed that the electronic properties of bisphenazine can be modulated with the type of peripheral substituent introduced.

The fluorescence emission spectra for compounds **1–5** are shown in Figure 2. The fluorescence spectra were normal-

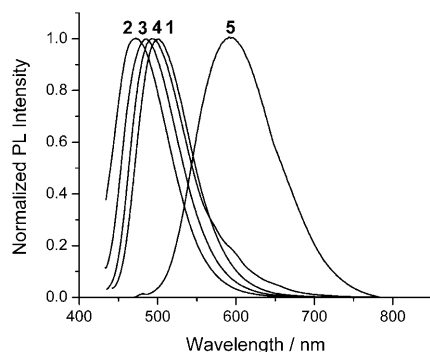


Figure 2. Photoluminescence spectra of compounds **1–5** (emission of compound **6** is identical to that of compound **5**). Excitation λ : 422 nm (**1** and **4**), 423 nm (**2** and **3**), and 418 nm (**5**).

ized at the emission maxima for comparison. The reduction of the optical energy gap seen in the UV-visible spectra was also manifested in fluorescence. As the HOMO–LUMO gap narrowed, the fluorescence wavelength became longer, which was clearly evident for these molecules. Note that the emission maxima of compounds **5** and **6** showed significantly large shifts to longer wavelengths compared to the other compounds. This observation was predicted by theory (Table 1).

The electrochemical properties of **1–6** were studied with cyclic voltammetry. All of the compounds studied showed quasi-reversible ($\Delta E_p \geq 90 \text{ mV n}^{-1}$) first reduction waves with peak splitting of 140 (**1**), 125 (**2**), 102 (**3**), 79 (**5**), and 86 mV (**6**). The peak splitting in compound **4** could not be calculated because the peak potentials were not clearly resolved.

Although the reductions of **5** and **6** appeared to be quasi-reversible processes, compound **6** exhibited a more reversible reduction, given that the cathodic and anodic peak currents were similar (Figure 3). A second reduction wave was

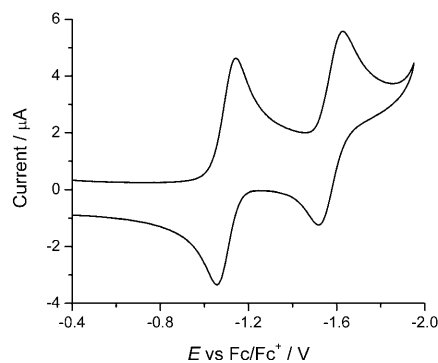


Figure 3. Cyclic voltammogram for the reduction of **6**. Scan rate = 100 mV s^{-1} .

observed in the voltammograms of both **5** and **6** since the presence of electron-withdrawing NO₂ groups increased the electron affinity of the molecules allowing the second wave to be easily seen. Compounds **1–3** may also have second reduction waves, however, they were not clearly observed owing to overlap with the solvent background. The onset of the reduction potential can be directly related to the electron affinity, or LUMO energy, of the molecule. Thus the onset of the first reduction wave was used to approximate the LUMO level (Table 1). The LUMO level was consistently lowered as the electron-withdrawing ability of the peripheral substituent increased from **2** < **3** < **1** < **5** = **6**. This result illustrates that further increase in the electron affinity of the whole system is possible by introducing a proper peripheral substituent to the bisphenazine core. To be a useful electron-transporting material, the electron-affinity of the molecule should be in the range of 2.7–3.4 eV for organic light-emitting diodes, and 3.8–4.5 eV for organic photovoltaics and field-effect transistors.^[14] The CV results imply that these compounds are potentially applicable for such opto-

electronics for *n*-channel function. The onset of the first oxidation wave can similarly be used to approximate the HOMO level of the molecule; however, oxidation potentials were not resolved for these compounds owing to irreproducibility and overlap with the solvent background. Thus, HOMO levels could not be directly estimated from CV. Instead, the HOMO values were calculated using the LUMO energies from CV and the optical energy gap (E_{gap}) values obtained from UV-visible spectroscopy^[15] (Table 1). In the case of compounds **5** and **6**, experimental HOMO energies were not determined by this method, as the energy gaps from UV-visible spectra were not resolved. Theoretical calculations were performed to further corroborate the experimental HOMO and LUMO energies and energy gap results obtained from cyclic voltammetry and UV-visible spectroscopy. Optimum geometries were calculated by using density functional theory (DFT)^[16] at the B3LYP/6-31G* level,^[17] and HOMO and LUMO energies and energy gaps were predicted by single point B3LYP/6-31+G*/B3LYP/6-31G* calculations. Compound **4** was not considered for comparable theoretical treatment because of limitations in suitably packaged basis sets for the element, iodine. Theoretical values are summarized and compared with experimental values in Table 1.

Although discrepancies between the experimental and theoretical energy levels were observed and expected, it is important to note that the theoretical calculations predicted that the LUMO levels would be lowered in the order $2 < 3 < 1 < 5 = 6$ which corresponded to the order seen experimentally. In addition, the lowering of the energy gap predicted from theoretical calculations was in the order $2 < 3 < 1 < 5 = 6$. This order was observed from UV-visible experiments ($2 < 3 < 4 < 1 < 5 = 6$).

The thermal properties of the final products were investigated by DSC. Compounds **2–4** (Figure 4 and Figure 5) had similar patterns, showing one endotherm (melting) and one exotherm (crystallization). The melting temperature showed a gradual increase from 83.1 °C to 105.4 °C to 121.9 °C from **2** to **4** to **3**. These results indicate that the intermolecular interactions become stronger in the series $2 < 4 < 3$. Compound **5** exhibited one endotherm at 140.5 °C and one exotherm at 115.0 °C with an additional small endotherm and exotherm at 168.9 °C and 157.5 °C, respectively, which may

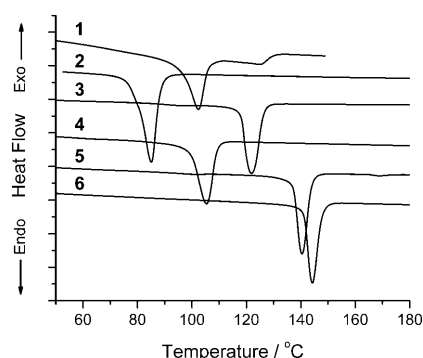


Figure 4. DSC thermograms of compounds **1–6** (second heating scan).

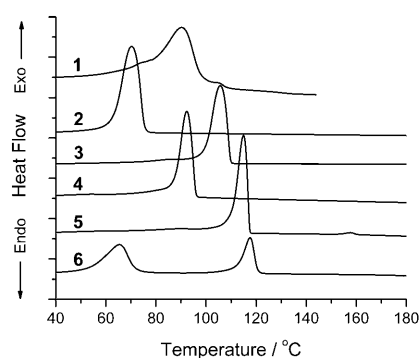


Figure 5. DSC thermograms of compounds **1–6** (second cooling scan).

indicate the existence of a liquid crystalline (LC) phase. The thermogram of compound **6** exhibited an endotherm at 144.2 °C and an exotherm at 117.5 °C similar to compound **5** with the absence of the exotherm/endotherm at higher temperatures. However, there was an additional exotherm at 65.5 °C. The heat of melting was equal to the sum of the heats of crystallization for the two exotherms. One possible explanation is that two different crystallites are being formed upon cooling, and both melt at the same temperature. The higher melting points of compounds **5** and **6** at 140.5 °C and 144.2 °C, respectively, could be attributed to the additional intermolecular interaction present between the NO₂ groups.^[18] The DSC scan of compound **1** showed one exotherm at 90.1 °C and the corresponding endotherm at 102.4 °C in a similar manner to compounds **2–4**. In addition, there was a second higher temperature endotherm at 124.8 °C. The second endotherm indicates the possible presence of an LC phase. The presence of a functional group, such as acetylene^[19] or NO₂,^[18] which can participate in an additional intermolecular interaction, may lead to the molecules arranging in such a way as to create a larger mesogen which could introduce an LC phase. We note that all of the transitions were reproducible over three heating/cooling scans.

In conjunction with molecular design approaches, assembly methodologies beyond simple spin-coating or casting have also been developed to fine-tune 1D structures including phase transfer,^[3b,20] solvent vapor annealing,^[3b,12n] injection,^[12j,21] precipitation,^[22] and organogelation.^[23] The 1D self-assembly of compounds **2–6** was studied using recrystallization from CH₂Cl₂ and a phase transfer (PT) method using two different binary solvent systems: CH₂Cl₂/hexane and CH₂Cl₂/methanol. The 1D assembly of compound **1** was not examined by these methods because detailed investigation of 1D nanostructure formation through organogelation was already demonstrated in the previous report.^[9] In the case of the recrystallization method, only compounds **5** and **6** formed self-assembled clusters. On the other hand, in the recrystallization of compound **2**, **3**, and **4**, a precipitation or a partial gelation with some precipitation was observed. The morphologies of the assembled clusters and their size distribution were compared based on the peripheral substituent (R¹), the alkyl chain length (R²=dodecyloxy or hexadecy-

loxy) and assembly method, and on the binary solvent systems used to induce the assemblies. First, the peripheral substituent effect on the self-assembly of compounds **2–5** was examined by comparing the morphologies of the nanoclusters obtained from the PT method (Figure 6).

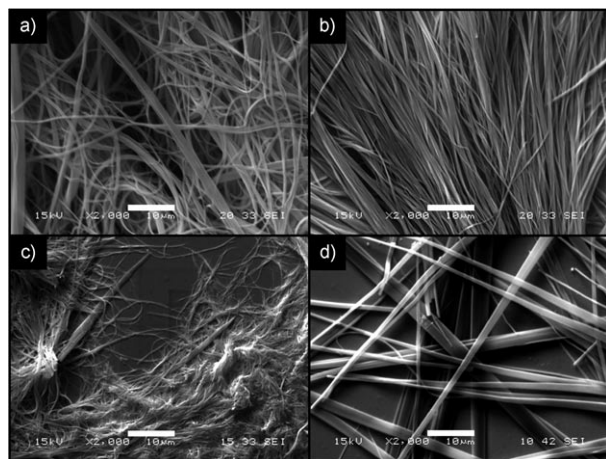


Figure 6. SEM images of PT assemblies of a) **2**, b) **3**, c) **4**, and d) **5** in CH_2Cl_2 /methanol. Scale bar: 10 μm .

Compounds **2–4** produced assembled structures in CH_2Cl_2 /methanol, while the CH_2Cl_2 /hexane system failed to induce any assembly, which may be attributed to some solubility of the compounds in the CH_2Cl_2 /hexane binary solvent system. However, compound **5** and **6** were assembled in both binary solvent systems and the morphologies of the 1D nanoclusters were somewhat dependent upon the solvent system used. This will be discussed later. Compound **2** formed endless, flexible, and flat nanofibers. Fiber bundles varied in size from ≈ 300 nm to 2 μm . In the case of compound **3**, fairly homogeneous nanofibers of approximately 600 nm in width were formed. The nanofibers formed were much straighter and shorter than those formed from compound **2**. Meanwhile, compound **4** formed thin and short fibers with very heterogeneous thickness and length distribution. This behavior may be due to irregular halogen-bonding interaction between iodine and imine nitrogen in neighboring molecules^[24] caused by steric *tert*-butyl side group, which may interfere with π - π interaction. The nitro substituted bisphenazine **5** formed straight nanofibers ranging in width from ≈ 900 nm to 3 μm . The fibers of **5** showed more of a belt-like morphology than the other compounds and were much less flexible than the nanofibers of **2** and **3**.

Unlike the other compounds, **5** and **6** produced very homogeneous micro- or nanobelts by recrystallization from CH_2Cl_2 (Figure 7). The width of the nanobelts obtained from **6** is much smaller than those of **5**. The widths of the microbelts obtained from **5** varied from ≈ 1 μm to 8 μm while those of **6** varied from ≈ 400 nm to 2 μm . The reason why **6** produced narrower nanobelts than **5** can be attributed in part to the higher solubility of **6** in CH_2Cl_2 leading to slower aggregation. It should be noted that recrystallization

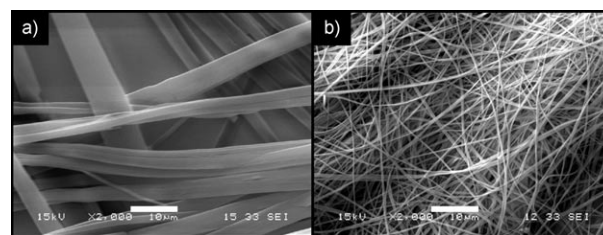


Figure 7. SEM images of a) **5** and b) **6** recrystallized from CH_2Cl_2 . Scale bar: 10 μm .

of **6** required overnight standing while **5** recrystallized within an hour.

In general, similar morphologies to those obtained from recrystallization were seen with the PT assemblies of **5** and **6** from CH_2Cl_2 /hexane and CH_2Cl_2 /methanol (Figure 8). The

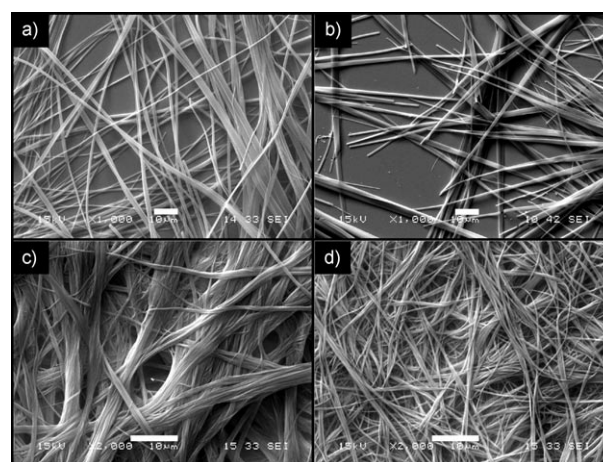


Figure 8. SEM images of the PT assemblies of **5** (a and b) and **6** (c and d). Binary solvent system for a and c: CH_2Cl_2 /hexane, for b and d: CH_2Cl_2 /methanol. Scale bar: 10 μm .

1D nanostructures of **5** obtained from CH_2Cl_2 /hexane ranged in width from ≈ 600 nm to 3 μm and those from CH_2Cl_2 /methanol were ≈ 900 nm to 3 μm . In the case of compound **6**, the width of the 1D clusters from CH_2Cl_2 /hexane ranged from ≈ 250 nm to 500 nm and those from CH_2Cl_2 /methanol were ≈ 600 nm to 900 nm. Three observations can be made from these results: 1) in the PT method, the nanoclusters formed from compound **5** are wider than those of **6** as previously described with those from recrystallization, 2) the width of the nanoclusters from the CH_2Cl_2 /hexane binary solvent system are smaller than those from CH_2Cl_2 /methanol, which is indicative of some solubility in the CH_2Cl_2 /hexane system, thus forming the more thermodynamic product, and 3) the PT assemblies of both **5** and **6** showed less lateral growth than recrystallization.

XRD studies were conducted on the 1D self-assembled clusters of compounds **2–6**. Although XRD alone is not sufficient to deduce the molecular packing in the 1D nanoclusters, the major purpose of this study was to determine if sig-

nificant π - π interactions were present in the assembled clusters. The typical distance for π - π stacking is 3.5 Å.^[25]

The XRD patterns of the nanofibers of **2**, **3**, and **4** obtained from the PT method using CH₂Cl₂/methanol were compared to determine the effect of the peripheral substituents on the 1D assembly. Although there are a number of peaks present in the patterns, the peaks of interest are near 23° (2 θ) corresponding to the π - π stacking distance along the fiber growth direction. In compound **2** (Figure 9a) the

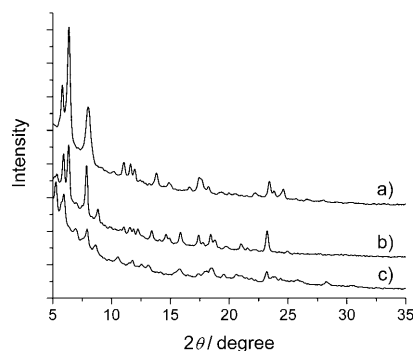


Figure 9. XRD patterns of PT assemblies of a) **2**, b) **3**, and c) **4** from CH₂Cl₂/methanol.

diffraction pattern showed sharp, intense peaks indicative of crystallinity in the assembled clusters. The peaks of interest correspond to *d*-spacings of 3.79, 3.73, and 3.61 Å. Compound **3** had a diffraction pattern similar to that of **2** with a more intense peak at 3.83 Å and a smaller peak at 3.57 Å. Compound **4** exhibited peaks similar to those found in **2** and **3**; however, they were of lower intensity and less defined and broader, indicating more amorphous character.

The XRD patterns of the recrystallized samples (compounds **5** and **6**) exhibited sharp, well-defined diffraction patterns indicative of high crystallinity. The peak of interest is at 22° (2 θ) corresponding to *d*-spacings of 3.96 Å for **5** (Figure 10a) and 4.02 Å for **6** (Figure 11a) which are larger than those of compounds **2-4**. This may be due to the tilting of the NO₂ groups from the plane of the heteroaromatic core which was predicted by theoretical calculations (Figure 12).

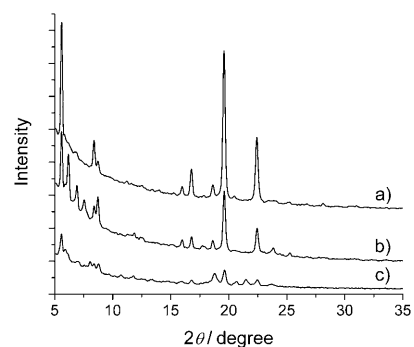


Figure 10. XRD patterns of **5** a) recrystallized from CH₂Cl₂, and b) PT from CH₂Cl₂/hexane and c) CH₂Cl₂/methanol.

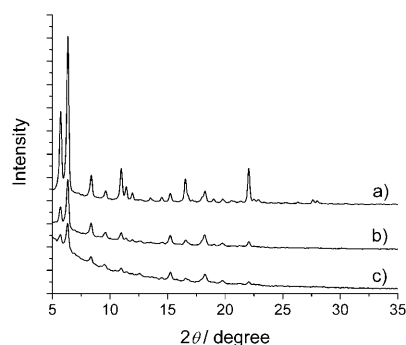


Figure 11. XRD patterns of **6** a) recrystallized from CH₂Cl₂, and b) PT from CH₂Cl₂/hexane and c) CH₂Cl₂/methanol.

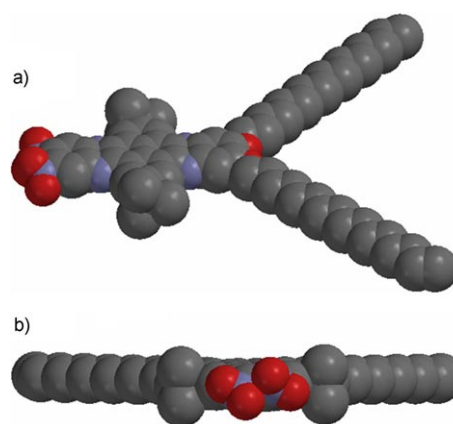


Figure 12. Space filling model of compound **5**^[26] optimized at the B3LYP/6-31G* level of theory: a) top view; b) side view from the nitro group. Color code: red-oxygen, violet-nitrogen, dark gray-carbon. Hydrogen atoms were omitted for clarity.

An interesting observation from the PT assembly with different binary solvent systems is that the diffraction patterns of the assembly from CH₂Cl₂/hexane (Figures 10b and 11b) are more similar to those of the recrystallized ones (Figures 10a, and 11a) than the PT with CH₂Cl₂/methanol (Figures 10c and 11c). During the process of PT, the molecules are forced to aggregate by a slow and continuous decrease in solubility, owing to the diffusion of a poor solvent into the solution. The solubility of the molecules in the binary solvent system should affect the morphology of assembled clusters. In the case of nitro substituted bisphenazines (**5** and **6**), the lower solubility of the compounds in methanol forces faster aggregation thus producing the less thermodynamic product.

The intermolecular π - π interaction in solid state was further investigated with UV-visible spectroscopy. Absorptions of two solid-state samples of compounds **2**, **3**, **5**, and **6** (self-assembled clusters by PT method from CH₂Cl₂/methanol and cast films) were recorded and compared with those in the solution state (Figure 13). In general, the self-assembled clusters showed significantly red-shifted absorption maxima compared to the absorption in the solution state. The cast films showed similar behavior with a less pronounced shift

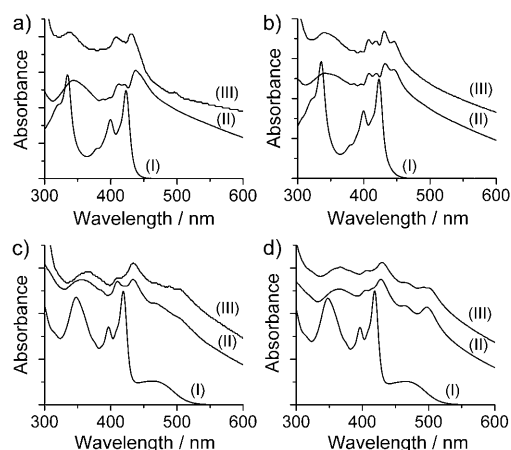


Figure 13. UV-visible spectra of compound a) **2**, b) **3**, c) **5**, and d) **6**: I) CHCl_3 , II) PT from CH_2Cl_2 /methanol, and III) cast film.

than the self-assembled clusters. In the case of compound **6** in CHCl_3 , $\lambda_{\text{max}} = 419 \text{ nm}$ was red-shifted to $\lambda = 428 \text{ nm}$ in the assembled clusters. In addition, the appearance of a new peak at $\lambda = 498 \text{ nm}$ in the self-assembled clusters (which was a shoulder in the solution state) suggests a possible *J*-aggregate formation. This trend is consistent with the previous observation from the absorption of nanofibers of compound **1** formed by organogelation.^[9] It is reasonable to assume that the systems in the present work adapt an off-face, stack geometry to accommodate bulky *tert*-butyl side groups. This result strongly supports intermolecular π -electron overlap in 1D self-assembled structures. UV-visible absorption of the self-assembled clusters of **4** was not obtained, owing to extensive aggregation.

Conclusions

In this paper, we demonstrated the effect of small peripheral substituents on the electronic property of the bisphenazine core. Among the substituents studied, the NO_2 group gave the most pronounced effect, lowering the LUMO energy level by $\approx 0.6 \text{ eV}$, and narrowing the HOMO–LUMO gap considerably when compared to H. Significant influence of these peripheral substituents was also observed in the morphology of self-assembled structures in terms of shape and size. Even with different types of peripheral substituents, the ability to produce 1D nanostructures was largely maintained. In addition, the length of alkoxy group, assembly method, and assembly condition influenced the fiber morphology significantly. This design approach illustrates a reasonable method for tailoring electronic and assembly properties of bisphenazine, a system that exhibits excellent potential for useful, future optoelectronic applications.

Acknowledgements

This work was partially supported by NSF EPSCoR Ring True III Award (EPS-0447416).

- [1] a) F. J. M. Hoeben, P. Jonkheijm, E. W. Meijer, A. P. H. J. Schenning, *Chem. Rev.* **2005**, *105*, 1491–1546; b) A. C. Grimsdale, K. Müllen, *Angew. Chem.* **2005**, *117*, 5732–5772; *Angew. Chem. Int. Ed.* **2005**, *44*, 5592–5629.
- [2] a) A. P. H. J. Schenning, E. W. Meijer, *Chem. Commun.* **2005**, 3245–3258; b) S. Xiao, J. Tang, T. Beetz, X. Guo, N. Tremblay, T. Siegrist, Y. Zhu, M. Steigerwald, C. Nuckolls, *J. Am. Chem. Soc.* **2006**, *128*, 10700–10701; c) A. L. Briseno, S. C. B. Mannsfeld, X. Lu, Y. Xiong, S. A. Jenekhe, Z. Bao, Y. Xia, *Nano Lett.* **2007**, *7*, 668–675.
- [3] a) B.-K. An, D.-S. Lee, J.-S. Lee, Y.-S. Park, H.-S. Song, S. Y. Park, *J. Am. Chem. Soc.* **2004**, *126*, 10232–10233; b) K. Balakrishnan, A. Datar, T. Naddo, J. Huang, R. Oitker, M. Yen, J. Zhao, L. Zang, *J. Am. Chem. Soc.* **2006**, *128*, 7390–7398; c) Y. Li, F. Li, H. Zhang, Z. Xie, W. Xie, H. Xu, B. Li, F. Shen, L. Ye, M. Hanif, D. Mab, Y. Ma, *Chem. Commun.* **2007**, 231–233; d) X. Zhang, X. Zhang, K. Zou, C.-S. Lee, S.-T. Lee, *J. Am. Chem. Soc.* **2007**, *129*, 3527–3532.
- [4] a) J. P. Hill, W. Jin, A. Kosaka, T. Fukushima, H. Ichihara, T. Shimomura, K. Ito, T. Hashizume, N. Ishii, T. Aida, *Science* **2004**, *304*, 1481–1483; b) Y. Yamamoto, T. Fukushima, Y. Suna, N. Ishii, A. Saeki, S. Seki, S. Tagawa, M. Taniguchi, T. Kawai, T. Aida, *Science* **2006**, *314*, 1761–1764; c) E. Lee, Y.-H. Jeong, J.-K. Kim, M. Lee, *Macromolecules* **2007**, *40*, 8355–8360; d) J.-K. Kim, E. Lee, Y.-H. Jeong, J.-K. Lee, W.-C. Zin, M. Lee, *J. Am. Chem. Soc.* **2007**, *129*, 6082–6083.
- [5] D. F. Perepichka, M. R. Bryce, *Angew. Chem.* **2005**, *117*, 5504–5507; *Angew. Chem. Int. Ed.* **2005**, *44*, 5370–5373.
- [6] a) S. C. Moratti, R. Cervini, A. B. Holmes, D. R. Baigent, R. H. Friend, N. C. Greenham, J. Grüner, P. J. Hamer, *Synth. Met.* **1995**, *71*, 2117–2120; b) A. Yassar, F. Demanze, A. Jaafari, M. E. Idrissi, C. Coupry, *Adv. Funct. Mater.* **2002**, *12*, 699–708; c) T. M. Pappenfus, M. W. Burand, D. E. Janzen, K. R. Mann, *Org. Lett.* **2003**, *5*, 1535–1538; d) M. M. Bader, R. Custelcean, M. D. Ward, *Chem. Mater.* **2003**, *15*, 616–618; e) B. A. Jones, M. J. Ahrens, M.-H. Yoon, A. Facchetti, T. J. Marks, M. R. Wasielewski, *Angew. Chem.* **2004**, *116*, 6523–6526; *Angew. Chem. Int. Ed.* **2004**, *43*, 6363–6366; f) T. M. Pappenfus, B. J. Hermanson, T. J. Helland, G. G. W. Lee, S. M. Drew, K. R. Mann, K. A. McGee, S. C. Rasmussen, *Org. Lett.* **2008**, *10*, 1553–1556.
- [7] a) S. Hiller, D. Schlettwein, N. R. Armstrong, D. Wöhler, *J. Mater. Chem.* **1998**, *8*, 945–954; b) Z. Bao, A. J. Lovinger, J. Brown, *J. Am. Chem. Soc.* **1998**, *120*, 207–208; c) D. Schlettwein, H. Graaf, J.-P. Meyer, T. Oekermann, N. I. Jaeger, *J. Phys. Chem. B* **1999**, *103*, 3078–3086; d) S. B. Heidenhain, Y. Sakamoto, T. Suzuki, A. Miura, H. Fujikawa, T. Mori, S. Tokito, Y. Taga, *J. Am. Chem. Soc.* **2000**, *122*, 10240–10241; e) Y. Sakamoto, S. Komatsu, T. Suzuki, *J. Am. Chem. Soc.* **2001**, *123*, 4643–4644; f) D. Schlettwein, K. Hesse, N. E. Gruhn, P. A. Lee, K. W. Nebesny, N. R. Armstrong, *J. Phys. Chem. B* **2001**, *105*, 4791–4800; g) B. A. Bench, A. Beveridge, W. M. Sharman, G. J. Diebold, J. E. van Lier, S. M. Gorun, *Angew. Chem.* **2002**, *114*, 773–776; *Angew. Chem. Int. Ed.* **2002**, *41*, 748–750; h) A. Facchetti, M.-H. Yoon, C. L. Stern, H. E. Katz, T. J. Marks, *Angew. Chem.* **2003**, *115*, 4030–4033; *Angew. Chem. Int. Ed.* **2003**, *42*, 3900–3903; i) S. P. Keizer, J. Mack, B. A. Bench, S. M. Gorun, M. J. Stillman, *J. Am. Chem. Soc.* **2003**, *125*, 7067–7085; j) U. Weiler, T. Mayer, W. Jaegermann, C. Kelting, D. Schlettwein, S. Makarov, D. Wöhler, *J. Phys. Chem. B* **2004**, *108*, 19398–19403; k) M.-S. Liao, T. Kar, S. M. Gorun, S. Scheiner, *Inorg. Chem.* **2004**, *43*, 7151–7161; l) M.-S. Liao, J. D. Watts, M.-J. Huang, S. M. Gorun, T. Kar, S. Scheiner, *J. Chem. Theory Comput.* **2005**, *1*, 1201–1210; m) R. Schmidt, M. M. Ling, J. H. Oh, M. Winkler, M. Könemann, Z. Bao, F. Würthner, *Adv. Mater.* **2007**, *19*, 3692–3695; n) H. Z. Chen, M. M. Ling, X. Mo, M. M. Shi, M. Wang, Z. Bao, *Chem. Mater.* **2007**, *19*, 816–824.

- [8] a) T. Yokoyama, S. Yokoyama, T. Kamikado, Y. Okuno, S. Mashiko, *Nature* **2001**, *413*, 619–621; b) M. M. S. Abdel-Mottaleb, G. Götz, P. Kilickiran, P. Bäuerle, E. Mena-Osteritz, *Langmuir* **2006**, *22*, 1443–1448; c) N. Wintjes, D. Bonifazi, F. Cheng, A. Kiebele, M. Stöhr, T. Jung, H. Spillmann, F. Diederich, *Angew. Chem.* **2007**, *119*, 4167–4170; *Angew. Chem. Int. Ed.* **2007**, *46*, 4089–4092; d) N. Wintjes, J. Hornung, J. Lobo-Checa, T. Voigt, T. Samuely, C. Thilgen, M. Stöhr, F. Diederich, T. A. Jung, *Chem. Eur. J.* **2008**, *14*, 5794–5802.
- [9] D.-C. Lee, K. K. McGrath, K. Jang, *Chem. Commun.* **2008**, 3636–3638.
- [10] a) J. Hu, D. Zhang, S. Jin, S. Z. D. Cheng, F. W. Harris, *Chem. Mater.* **2004**, *16*, 4912–4915; b) B. R. Kaafarani, L. A. Lucas, B. Wex, G. E. Jabbour, *Tetrahedron Lett.* **2007**, *48*, 5995–5998; c) D.-C. Lee, K. Jang, K. K. McGrath, R. Uy, K. A. Robins, D. W. Hatchett, *Chem. Mater.* **2008**, *20*, 3688–3695; d) B. Gao, M. Wang, Y. Cheng, L. Wang, X. Jing, F. Wang, *J. Am. Chem. Soc.* **2008**, *130*, 8297–8306; e) L. A. Lucas, D. M. DeLongchamp, L. J. Richter, R. J. Kline, D. A. Fischer, B. R. Kaafarani, G. E. Jabbour, *Chem. Mater.* **2008**, *20*, 5743–5749.
- [11] T. Yamamoto, T. Maruyama, Z. Zhou, T. Ito, T. Fukuda, Y. Yoneda, F. Begam, T. Ikeda, S. Sasaki, H. Takezoe, A. Fukuda, K. Kubota, *J. Am. Chem. Soc.* **1994**, *116*, 4832–4845.
- [12] a) E. Keinan, S. Kumar, S. P. Singh, R. Ghirlando, E. J. Wachtel, *Liq. Cryst.* **1992**, *11*, 157–173; b) S. Kumar, E. J. Wachtel, E. Keinan, *J. Org. Chem.* **1993**, *58*, 3821–3827; c) S. Kumar, D. S. S. Rao, S. K. Prasad, *J. Mater. Chem.* **1999**, *9*, 2751–2754; d) K. Pieterse, P. A. van Hal, R. Kleppinger, J. A. J. M. Vekemans, R. A. J. Janssen, E. W. Meijer, *Chem. Mater.* **2001**, *13*, 2675–2679; e) V. Lemaury, D. A. da Silva Filho, V. Coropceanu, M. Lehmann, Y. Geerts, J. Piris, M. G. Debije, A. M. van de Craats, K. Senthilkumar, L. D. A. Siebbeles, J. M. Warman, J.-L. Brédas, J. Cornil, *J. Am. Chem. Soc.* **2004**, *126*, 3271–3279; f) J. Kadam, D. F. J. Faul, U. Scherf, *Chem. Mater.* **2004**, *16*, 3867–3871; g) M. Lehmann, V. Lemaury, J. Cornil, J.-L. Brédas, S. Goddard, I. Grizzi, Y. Geerts, *Tetrahedron* **2004**, *60*, 3283–3291; h) M. Lehmann, G. Kestemont, R. G. Aspe, C. Buess-Herman, M. H. J. Koch, M. G. Debije, J. Piris, M. P. de Haas, J. M. Warman, M. D. Watson, V. Lemaury, J. Cornil, Y. H. Geerts, R. Gearba, D. A. Ivanov, *Chem. Eur. J.* **2005**, *11*, 3349–3362; i) T.-H. Chang, B.-R. Wu, M. Y. Chiang, S.-C. Liao, C. W. Ong, H.-F. Hsu, S.-Y. Lin, *Org. Lett.* **2005**, *7*, 4075–4078; j) K. Balakrishnan, A. Datar, R. Oitker, H. Chen, J. Zuo, L. Zang, *J. Am. Chem. Soc.* **2005**, *127*, 10496–10497; k) T. Ishi-I, K. Yaguma, R. Kuwahara, Y. Taguri, S. Mataka, *Org. Lett.* **2006**, *8*, 585–588; l) T. Ishi-I, H. Tashiro, R. Kuwahara, S. Mataka, T. Yoshihara, S. Tobita, *Chem. Lett.* **2006**, *35*, 158–159; m) Y. Li, Y. Li, J. Li, C. Li, X. Liu, M. Yuan, H. Liu, S. Wang, *Chem. Eur. J.* **2006**, *12*, 8378–8385; n) A. Datar, R. Oitker, L. Zang, *Chem. Commun.* **2006**, 1649–1651; o) Y. Che, A. Datar, X. Yang, T. Naddo, J. Zhao, L. Zang, *J. Am. Chem. Soc.* **2007**, *129*, 6354–6355; p) Y. Che, A. Datar, K. Balakrishnan, L. Zang, *J. Am. Chem. Soc.* **2007**, *129*, 7234–7235.
- [13] E. Bundgaard, F. C. Krebs, *Macromolecules* **2006**, *39*, 2823–2831.
- [14] a) A. P. Kulkarni, C. J. Tonzola, A. Babel, S. A. Jenekhe, *Chem. Mater.* **2004**, *16*, 4556–4573; b) C. J. Tonzola, M. M. Alam, S. A. Jenekhe, *Macromolecules* **2005**, *38*, 9539–9547.
- [15] Y. Fogel, M. Kastler, Z. Wang, D. Andrienko, G. J. Bodwell, K. Müllen, *J. Am. Chem. Soc.* **2007**, *129*, 11743–11749.
- [16] A. D. Becke, *J. Chem. Phys.* **1993**, *98*, 5648–5652.
- [17] Gaussian 03, Revision C.02, M. J. Frisch, G. W. Trucks, H. B. Schlegel, G. E. Scuseria, M. A. Robb, J. R. Cheeseman, J. A. Montgomery, Jr., T. Vreven, K. N. Kudin, J. C. Burant, J. M. Millam, S. S. Iyengar, J. Tomasi, V. Barone, B. Mennucci, M. Cossi, G. Scalmani, N. Rega, G. A. Petersson, H. Nakatsuji, M. Hada, M. Ehara, K. Toyota, R. Fukuda, J. Hasegawa, M. Ishida, T. Nakajima, Y. Honda, O. Kitao, H. Nakai, M. Klene, X. Li, J. E. Knox, H. P. Hratchian, J. B. Cross, V. Bakken, C. Adamo, J. Jaramillo, R. Gomperts, R. E. Stratmann, O. Yazyev, A. J. Austin, R. Cammi, C. Pomelli, J. W. Ochterski, P. Y. Ayala, K. Morokuma, G. A. Voth, P. Salvador, J. J. Dannenberg, V. G. Zakrzewski, S. Dapprich, A. D. Daniels, M. C. Strain, O. Farkas, D. K. Malick, A. D. Rabuck, K. Raghavachari, J. B. Foresman, J. V. Ortiz, Q. Cui, A. G. Baboul, S. Clifford, J. Cioslowski, B. B. Stefanov, G. Liu, A. Liashenko, P. Piskorz, I. Komaromi, R. L. Martin, D. J. Fox, T. Keith, M. A. Al-Laham, C. Y. Peng, A. Nanayakkara, M. Challacombe, P. M. W. Gill, B. Johnson, W. Chen, M. W. Wong, C. Gonzalez, J. A. Pople, Gaussian, Inc., Wallingford CT, **2004**.
- [18] a) K. Wozniak, H. He, J. Minowski, W. Jones, E. Grechs, *J. Phys. Chem.* **1994**, *98*, 13755–13765; b) E. Gagnon, T. Maris, K. E. Malyz, J. D. Wuest, *Tetrahedron* **2007**, *63*, 6603–6613.
- [19] J. C. D. Brand, G. Eglinton, J. F. Morman, *J. Chem. Soc.* **1960**, 2526–2533.
- [20] A. L. Briseno, S. C. B. Mannsfeld, C. Reese, J. M. Hancock, Y. Xiong, S. A. Jenekhe, Z. Bao, Y. Xia, *Nano Lett.* **2007**, *7*, 2847–2853.
- [21] a) D. M. Vriezema, A. Kros, R. de Gelder, J. J. L. M. Cornelissen, A. E. Rowan, R. J. M. Nolte, *Macromolecules* **2004**, *37*, 4736–4739; b) H. Katagi, H. Kasai, S. Okada, H. Oikawa, H. Matsuda, H. Nakanishi, *J. Macromol. Sci. Pure Appl. Chem.* **1997**, *34*, 2013–2024.
- [22] A. L. Briseno, S. C. B. Mannsfeld, P. J. Shamberger, F. S. Ohuchi, Z. Bao, S. A. Jenekhe, Y. Xia, *Chem. Mater.* **2008**, *20*, 4712–4719.
- [23] a) P. Terech, R. G. Weiss, *Chem. Rev.* **1997**, *97*, 3133–3160; b) D. J. Abdallah, R. G. Weiss, *Adv. Mater.* **2000**, *12*, 1237–1247; c) A. Ajayaghosh, V. K. Praveen, *Acc. Chem. Res.* **2007**, *40*, 644–656.
- [24] a) T. Uchida, K. Kimura, *Acta Crystallogr. Sect. C* **1984**, *40*, 139–140; b) A. C. B. Lucassen, T. Zubkov, L. J. W. Shimonb, M. E. van der Boom, *CrystEngComm* **2007**, *9*, 538–540; c) T. Shirman, D. Freeman, Y. D. Posner, I. Feldman, A. Facchetti, M. E. van der Boom, *J. Am. Chem. Soc.* **2008**, *130*, 8162–8163; d) D. Cinčić, T. Friščić, W. Jones, *Chem. Mater.* **2008**, *20*, 6623–6626.
- [25] L. Schmidt-Mende, A. Fechtenkotter, K. Müllen, E. Moons, R. H. Friend, J. D. MacKenzie, *Science* **2001**, *293*, 1119–1122.
- [26] Spartan '04, Wavefunction, Inc. Irvine.

Received: October 16, 2008

Published online: February 24, 2009